Received: 5 February 2021 | Revised: 11 June 2021 | Accepted: 1 August 2021

DOI: 10.1002/aic.17393

PROCESS SYSTEMS ENGINEERING

AIChE JOURNAL

Globally optimal synthesis of heat exchanger networks. Part III: Non-isothermal mixing in minimal and non-minimal networks

Chenglin Chang[1] | Zuwei Liao[2] | André L. H. Costa[3] | Miguel J. Bagajewicz[3,4]

[1]Zhejiang Provincial Key Laboratory of Advanced Chemical Engineering Manufacture Technology, College of Chemical and Biological Engineering, Zhejiang University, Hangzhou, China

[2]State Key Laboratory of Chemical Engineering, College of Chemical and Biological Engineering, Zhejiang University, Hangzhou, China

[3]Institute of Chemistry, Rio de Janeiro State University (UERJ), Rio de Janeiro, Brazil

[4]School of Chemical, Biological and Materials Engineering, University of Oklahoma, Norman, Oklahoma, USA

Correspondence
Zuwei Liao, State Key Laboratory of Chemical Engineering, College of Chemical and Biological Engineering, Zhejiang University, Hangzhou 310027, China.
Email: liaozw@zju.edu.cn

Funding information
China Postdoctoral Science Foundation, Grant/Award Numbers: 2019TQ0275, 2020M671723; National Council for Scientific and Technological Development (CNPq), Grant/Award Number: Process 310390/2019-2; National Natural Science Foundation of China, Grant/Award Numbers: 21822809, 21978256, 22008210; Prociência Program (UERJ), Grant/Award Number: PAPD Program; the Foundation of State Key Laboratory of High-efficiency Utilization of Coal and Green Chemical Engineering, Grant/Award Number: 2018-K23

Abstract

In this work, the enumeration algorithms presented in Parts I and II for the globally optimal synthesis of minimal and non-minimal heat exchanger networks are extended to consider non-isothermal mixing. New mathematical models, including non-isothermal mixing constraints, are proposed to target the bounds of energy consumption and the binding exchanger minimum approximation temperature. These models are solved using the algorithms, which involve solving systems of equations instead of mathematical programming. Three global optimization strategies are proposed to optimize each enumerated structure, involving the use of a global solver directly, or the use of a Golden Search based on energy consumption and a flowrate optimization model considering non-isothermal mixing. The flowrate optimization model is reformulated as a convex problem, which is solved by using nonlinear programming or a mathematical programming-free methodology, that is, solving Karush–Kuhn–Tucker equations. A new Global Optimum Search Algorithm is developed and examples are tested comparing different optimization strategies.

KEYWORDS
global optimum search algorithm, heat exchanger networks, non-isothermal mixing

1 | INTRODUCTION

The synthesis of heat exchanger network (HEN) is a well-known research topic in Process Systems Engineering. Numerous design technologies and methods have been developed with extensive application to industrial practice, as stated in review articles[1,2] and research publications,[3,4] to name a few. Of all the previous works on HEN synthesis, the approach that gains dominance is the one where a superstructure is proposed together with the formulation of a mixed-integer nonlinear model (MINLM), which can be solved using mixed-integer nonlinear programming (MINLP) procedures,[5,6] many times using decompositions,[7,8] or stochastic-based methods (meta-heuristics-based methods), such as genetic algorithms,[9,10] simulated algorithms,[11,12] particle swarm optimization,[13,14] hybridization between different algorithms,[15,16] etc. We do not elaborate further on the literature review of the stochastic-based methods, which cannot guarantee optimality, much less global optimality, and in general need specialized parameter tuning for a good computational performance. In turn, we concentrate on the use of the MINLP procedures in this work.

The two most popular superstructures used in previous works are, respectively, the generalized superstructure proposed by Floudas et al.[17] and the stage-wise superstructure proposed by Yee and Grossmann.[18] Zamora and Grossmann[19] simplified HEN synthesis with the assumption of no stream splits using stage-wise superstructure. Branch-and-bound (BB) and outer approximation (OA) approaches were combined to propose a global optimization algorithm. Bergamini et al.[20] derived additional constraints from physical insights that tightened the stage-wise HEN model. Piecewise relaxation technologies were used to obtain the under-estimators of exchanger areas in their proposed global optimization algorithm. Bogataj and Kravanja[21] proposed an alternative global optimization strategy for HEN synthesis by introducing aggregated substructures. Convex approximation and under-estimators were incorporated into the strategy to decrease the gaps between lower and upper bounds. Faria et al.[22] applied a bound contraction procedure, namely RYSIA, to solve the stage-wise superstructure model. Both small- and medium-scale cases were tested and global optimality could be guaranteed. Mistry and Misener[23] provided the proof to demonstrate that the reverse logarithmic mean temperature difference (LMTD) is convex. The original HEN model was approximated using a mixed-integer linear model (MILM), which iteratively run and converged to the global optimum of the original problem. Beck and Hofmann[24] proposed several useful measures to tighten the stage-wise HEN model including additional inequality constraints and tighter variable bounds. These measures could help solvers to find the global optimum and decrease the duality gaps significantly. However, all these above discussed models are based on the assumption of isothermal mixing, which in general overestimates heat exchanger areas and restrict the trade-offs between capital and operational costs.

Non-isothermal mixing is a well-known topic of HEN synthesis. Huang et al.[25] extended the bounds of the sub-streams' temperatures and added logical constraints for non-isothermal mixing. They evaluated different LMTD approximations and proposed several ways to handle LMTD exactly. Huang and Karimi[26] established a multistage superstructure including cross flows which combined the superstructures of Floudas et al.[17] and Yee and Grossmann.[18] Their multistage superstructure included additional network configurations but featured a more complex mathematical model. Huang and Karimi[27] proposed a tailored-search strategy that repeatedly revived an improved OA algorithm to establish simpler and smaller perturbations for the master problems. However, the OA algorithm solved the HEN model in sequential steps and could not guarantee global optimality. Björkand and Westerlund[28] convexified the nonlinear term in stage-wise HEN model with non-isothermal mixing. A global optimization strategy was developed, relying on the lower bounds provided by the convex sub-problems that were created by piecewise linear relaxation technologies. Kim and Bagajewicz[29] used a new generalized superstructure, which was modified from Floudas et al.,[17] to consider more possible stream matches, splits, bypasses, and non-isothermal mixing. The authors proposed a useful bound contraction procedure (RYSIA) to globally solve HEN models without using BB steps. Kim et al.[30] constructed a stages/substages superstructure to synthesize HENs with non-isothermal mixing. Their model allowed more commonly acceptable networks than the topology configurations of the generalized superstructures featuring disorganized branches and presenting challenges in practice.

The aforementioned HEN works about MINLP procedures are comparatively summarized in Table A1 of Supporting Information-Part A. It should be mentioned that all the solution strategies used by these works exhibit computational difficulties when applied to medium and large problems either with isothermal or non-isothermal mixing.

Departing from the exclusive use of MINLP procedures, in Parts I and II of this research,[31,32] we proposed a novel solution procedure based on the exhaustive enumeration and smart enumeration of network structures, aided by low demanding mathematical programming procedures. The smart enumeration that we refer to is Option 1 in our Parts I and II, where a lower bound (LB) model is run with a stopping criteria to generate HEN network structures one by one until the LB is larger than the incumbent best value. The important point is that our exhaustive and smart enumeration algorithms are both capable of solving different sizes of problems to global optimality, even medium- and large-size ones. However, all the models in our Parts I and II are linear based on isothermal mixing assumption that may restrict the holistic trade-offs between the capital investment and energy recovery. In another words, the algorithms presented in our Parts I and II cannot be directly applied to synthesize HENs with non-isothermal mixing. Hence, there is necessity and incentive to develop new mathematical models by adding the constraints of non-isothermal mixing and improve our previous enumeration algorithms to solve HEN synthesis problems with non-isothermal mixing to global optimality.

In this work, we extend the enumeration algorithms presented in our Parts I and II to develop a new Global Optimum Search Algorithm to further consider non-isothermal mixing for minimal and non-minimal HENs synthesis. Similar to previous algorithms, we recursively run *PLB* and *PSTR* models (see Parts I and II) to exhaustively enumerate different HEN structures (all feasible stream matches) using a combination of MILMs solved by mixed-integer linear programming (MILP) procedure to obtain HEN candidate structures. For each structure, the network's total annualized cost (TAC) is optimized for the energy (total hot utility demand) and binding exchanger minimum approximation temperature (EMAT) using Golden Search strategy and direct computation of exchanger area. Compared with Parts I and II, the changes of the developed Global Optimum Search Algorithm in this work are described as follows.

1. New mathematical models, including the nonlinear constraints related to the non-isothermal mixing, are established to obtain the lower and upper bounds of energy consumption, as well as the locations and bounds of the binding EMAT for the HEN structures. Several sub-algorithms are developed to solve these NLMs to global optimality.
2. Three optimization strategies are proposed to optimize each enumerated structure:
   - Strategy 1: A global solver is employed for each enumerated structure using problems *PLB* and *PSTR* (see Parts I and II)

without using a Golden Search as it was already done in Parts I and II.

- Strategy 2: Use Golden Search to optimize the energy consumption and binding EMAT. However, when there exist stream splits in the structure, the flowrate capacities of stream splits must be optimized to handle non-isothermal mixing. This flowrate optimization is done by running a NLM.
- Strategy 3: Same as Strategy 2, but instead of solving a nonlinear problem, we solve the Karush–Kuhn–Tucker (KKT) equations of the NLM.

Small- and medium-size examples, the most common in industrial practices, are solved in competitive time. In the case of large-scale problems (15–39 streams), global optimality is also achieved, but the computational time increases. Two issues are worth noticing for large-scale examples:

1. We know that these problems had been near-globally solved by using stochastic or metaheuristic procedures, although tuning of parameters is likely to be needed;
2. We know that without good initial points global solvers (BARON and ANTIGONE) many times fail while other solution procedures like RYSIA have memory and time problems. Hence, having a tool for global optimization albeit time-consuming is an advance. Future work will be aimed to reduce the computational time.

The rest of this article is structured as follows. First, three global optimization strategies are proposed. Then, we describe some properties of HEN with non-isothermal mixing and prove that the NLP optimizing the flowrate capacities of stream splits can be reformulated as a convex problem. Following, the formulations of new mathematical models and sub-algorithms are presented. Next, a Global Optimum Search Algorithm is developed. Finally, 19 examples are tested and conclusions follow.

2 | GLOBAL OPTIMIZATION STRATEGIES

Three global optimization strategies that rely on enumerating HEN structures by recursively running *PLB* or *PSTR* models (see Part I) for exhaustive enumeration are presented below. As discussed in Parts I and II, global optimality is achieved in both cases (*PLB* and *PSTR*).

1. Strategy 1: For each fixed structure being enumerated, initialize a global solver (we used BARON) with the solution results of the enumeration procedure (*PLB* or *PSTR*), and solve the resulting NLP model (see Supporting Information-Part B) considering non-isothermal mixing to global optimality. This strategy avoids the use of Golden Search. BARON is known to exhibit convergence problems in the case wherein the integer variables are not fixed (i.e., the HEN structure is not fixed) and/or when poor initial values are given. However, we find that, after fixing the integers, solving the resulting NLP using BARON with fixed integer variables works well in small- and medium-scale examples but fails in large-scale ones.
2. Strategy 2: Proceed with the Golden Search algorithms developed in Parts I and II, for each value of the energy consumption and binding EMAT, solve an NLM to minimize area cost only for the heat exchangers which are involved in stream splits. These are isolated HEN structures consisting of a few heat exchangers, a result of limiting the total number of exchangers.
3. Strategy 3: Proceed with the Golden Search algorithms developed in Parts I and II, solve the system of equations based on the KKT conditions corresponding to the aforementioned NLM.

It should be pointed out that the original model optimizing the flowrate capacities of stream split (area cost minimization) is a non-convex NLP. Indeed, this problem can be solved to global optimality by BARON, but it usually requires long solution time especially when solving large-size cases. Therefore, we reformulate the original NLP as a convex NLM, which has one and only one local optimum that is, in fact, the global solution. This convex NLM can be easily solved to global optimality either using BARON (Strategy 2) or by solving its KKT equations (Strategy 3). Note that solving the system of KKT equations (Strategy 3) is faster than using gradient-based NLP (Strategy 2), especially in large-scale problems. In Examples section, we compare different Strategies and find that Strategy 3 exhibits computational advantages in large-size examples. We remark that Strategy 3 is a mathematical programming-free methodology.

In the next section, we prove that the NLM corresponding to Strategies 2 and 3 is a convex problem. Then, the equations of KKT conditions for Strategy 3 are presented.

It is worth mentioning that Strategy 3, aside from the generation of HEN structures, can be implemented without any other tools than a solver of systems of equations, with no mathematical programming involved. Moreover, knowing that the candidate HEN structures can be generated algorithmically by exploiting graph theory properties, our Strategy 3 can potentially be the first mathematical programming-free procedure for globally optimal HEN synthesis.

3 | CONVEX MODEL FOR FLOWRATE OPTIMIZATION IN STREAM SPLITS

Consider a hot stream and a cold stream involved in splits, as depicted in Figure 1.

Binary parameters $Y^H_{i,k}$ and $Y^C_{j,k}$ are defined to, respectively, denote whether hot stream i and cold stream j are split or not at stage k. For a HEN structure, the values of binary variables $z_{i,j,k}$, zhu_j, and zcu_i that represent the existence of heat exchangers are given, and they are written as $\widehat{z}_{i,j,k}$, $\widehat{z}hu_j$, and $\widehat{z}cu_i$. Then, the values of $Y^H_{i,k}$ and $Y^C_{j,k}$ are assigned as follows.

$$Y^H_{i,k} = \begin{cases} 1 & \sum_{j \in CP} \widehat{z}_{i,j,k} > 1 \\ 0 & \text{Otherwise} \end{cases} \qquad \forall i \in HP, k \in ST \tag{1}$$

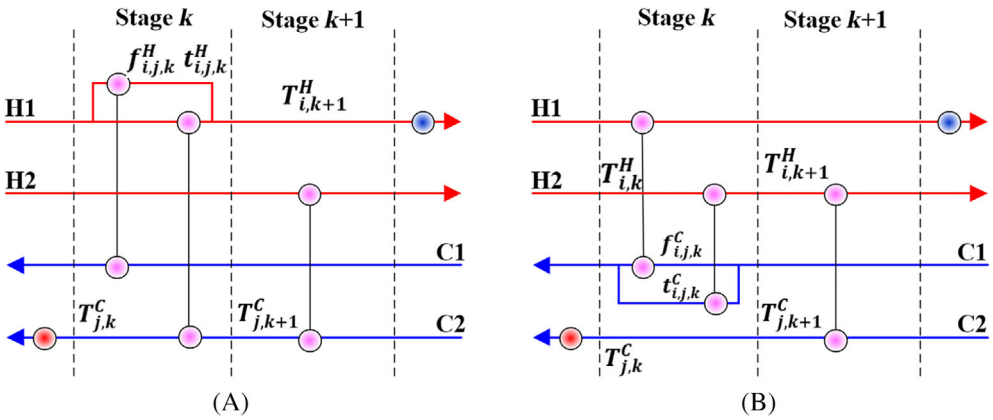

FIGURE 1 Stream splits and nomenclature: (A) Hot stream split and (B) cold stream split

$$Y^C_{j,k}=\begin{cases}1 & \sum_{i\in HP}\hat{z}_{i,j,k}>1\\ 0 & \text{Otherwise}\end{cases}\qquad \forall j\in CP,k\in ST \tag{2}$$

As demonstrated in Part I, the heat loads ($\hat{q}_{i,j,k}$, $\hat{q}hu_j$, and $\hat{q}cu_i$) for a minimum structure (MSTR) network (minimal network) are unique once energy consumption ($\hat{E}$) is fixed. The same can be said in the case of a non-MSTR network (non-minimal network) with the fixed hot utility consumption (energy) and fixed binding EMAT (see Part II). For minimal and non-minimal HENs with fixed energy consumption and fixed binding EMAT, the heat loads of all exchangers are fixed and the stream temperatures at stages are also fixed, and each stage can be solved independently of the others. Hence, of those, only the ones that have splits demand a NLM (flowrate optimization) to minimize area cost.

We recall that the stream temperatures at each stage upon mixing $\hat{T}^H_{i,k}$ and $\hat{T}^C_{j,k}$ are fixed parameters because of the overall energy balance for each stage. This is shown in Figure 2, which depicts instances of MSTR and non-MSTR networks with the fixed energy consumption and fixed binding EMAT respectively.

As in previous research, the cost of a heat exchanger is given by $C_{i,j,k}=\hat{a}\hat{z}_{i,j,k}+\hat{b}\hat{A}^{\hat{c}}_{i,j,k}$. Since the integers ($\hat{z}_{i,j,k}$) are fixed parameters in this problem, the objective function can be reduced to minimizing the sum of exchanger area costs ($\hat{b}\hat{A}^{\hat{c}}_{i,j,k}$). Here, the constant $\hat{b}$ is generally independent of exchanger area, and the objective can be set as minimizing the sum of concave terms ($\hat{A}^{\hat{c}}_{i,j,k}$). In addition, without loss of generality, we use the Paterson approximation[33] for LMTD since it makes the proof of convexity easier. The original flowrate optimization model (nonlinear) called *PS1* is the following:

$$Min\left\{\sum_{\substack{i\in HP\\Y^H_{i,k}=1}}\sum_{\substack{j\in CP\\Y^C_{j,k}=1}}\sum_{\substack{k\in ST\\\hat{z}_{i,j,k}=1}}\hat{A}^{\hat{c}}_{i,j,k}+\sum_{\substack{i\in HP\\Y^H_{i,k}=1}}\sum_{\substack{j\in CP\\Y^C_{j,k}=0}}\sum_{\substack{k\in ST\\\hat{z}_{i,j,k}=1}}\hat{A}^{\hat{c}}_{i,j,k}+\sum_{\substack{i\in HP\\Y^H_{i,k}=0}}\sum_{\substack{j\in CP\\Y^C_{j,k}=1}}\sum_{\substack{k\in ST\\\hat{z}_{i,j,k}=1}}\hat{A}^{\hat{c}}_{i,j,k}\right\} \tag{3}$$

$$\sum_{j\in CP,\hat{z}_{i,j,k}=1}f^H_{i,j,k}-Fcp^H_i=0\qquad \forall i\in HP,k\in ST,Y^H_{i,k}=1 \tag{4}$$

$$\sum_{i\in HP,\hat{z}_{i,j,k}=1}f^C_{i,j,k}-Fcp^C_j=0\qquad \forall j\in CP,k\in ST,Y^C_{j,k}=1 \tag{5}$$

$$\hat{q}_{i,j,k}=f^H_{i,j,k}\left(\hat{T}^H_{i,k}-t^H_{i,j,k}\right)\qquad \forall i\in HP,j\in CP,k\in ST,\hat{z}_{i,j,k}=1,Y^H_{i,k}=1 \tag{6}$$

$$\hat{q}_{i,j,k}=f^C_{i,j,k}\left(t^C_{i,j,k}-\hat{T}^C_{j,k+1}\right)\qquad \forall i\in HP,j\in CP,k\in ST,\hat{z}_{i,j,k}=1,Y^C_{j,k}=1 \tag{7}$$

$$\Delta t^C_{i,j,k}=t^H_{i,j,k}-\hat{T}^C_{j,k+1}\qquad \forall i\in HP,j\in CP,k\in ST,\hat{z}_{i,j,k}=1,Y^H_{i,k}=1 \tag{8}$$

$$\Delta t^H_{i,j,k}=\hat{T}^H_{i,k}-t^C_{i,j,k}\qquad \forall i\in HP,j\in CP,k\in ST,\hat{z}_{i,j,k}=1,Y^C_{j,k}=1 \tag{9}$$

$$\hat{q}_{i,j,k}\hat{U}^{-1}_{i,j}A^{-1}_{i,j,k}-\frac{2}{3}\sqrt{\Delta t^C_{i,j,k}\Delta t^H_{i,j,k}}-\frac{\Delta t^C_{i,j,k}}{6}-\frac{\Delta t^H_{i,j,k}}{6}\le 0 \tag{10}$$
$$\forall i\in HP,j\in CP,k\in ST,\hat{z}_{i,j,k}=1,Y^H_{i,k}=1,Y^C_{j,k}=1$$

$$\hat{q}_{i,j,k}\hat{U}^{-1}_{i,j}A^{-1}_{i,j,k}-\frac{2}{3}\sqrt{\left(\hat{T}^H_{i,k}-\hat{T}^C_{j,k}\right)\Delta t^C_{i,j,k}}-\frac{\hat{T}^H_{i,k}-\hat{T}^C_{j,k}}{6}-\frac{\Delta t^C_{i,j,k}}{6}\le 0 \tag{11}$$
$$\forall i\in HP,j\in CP,k\in ST,\hat{z}_{i,j,k}=1,Y^H_{i,k}=1,Y^C_{j,k}=0$$

$$\hat{q}_{i,j,k}\hat{U}^{-1}_{i,j}A^{-1}_{i,j,k}-\frac{2}{3}\sqrt{\left(\hat{T}^H_{i,k+1}-\hat{T}^C_{j,k+1}\right)\Delta t^H_{i,j,k}}-\frac{\hat{T}^H_{i,k+1}-\hat{T}^C_{j,k+1}}{6}-\frac{\Delta t^H_{i,j,k}}{6}\le 0$$
$$\forall i\in HP,j\in CP,k\in ST,\hat{z}_{i,j,k}=1,Y^H_{i,k}=0,Y^C_{j,k}=1 \tag{12}$$

$$\Delta t^C_{i,j,k}\ge EMAT_{Min}\qquad \forall i\in HP,j\in CP,k\in ST,\hat{z}_{i,j,k}=1,Y^H_{i,k}=1 \tag{13}$$

$$\Delta t^H_{i,j,k}\ge EMAT_{Min}\qquad \forall i\in HP,j\in CP,k\in ST,\hat{z}_{i,j,k}=1,Y^C_{j,k}=1 \tag{14}$$

In the above model, we define variables for both the heat capacity flowrates and temperatures of the stream splits: $f^H_{i,j,k}$ and $t^H_{i,j,k}$ for hot stream; $f^C_{i,j,k}$ and $t^C_{i,j,k}$ for cold stream. Note that Equations (13) and (14) are demanded because the temperatures involved are variables. Model *PS1* in the current form is a nonconvex model that shows increased computational effort in large-size cases. This is because the

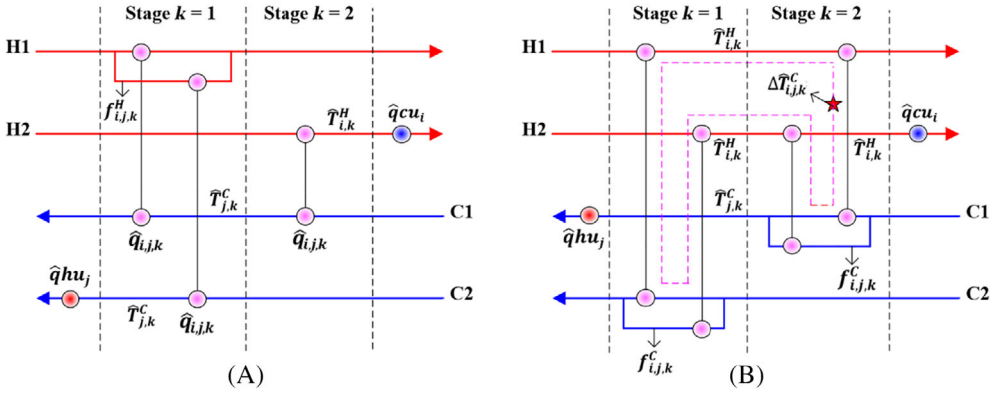

FIGURE 2 HENs with unique heat loads: (A) Minimal network and (B) non-minimal network

objective function is concave ($\hat{c}$ is usually smaller than one) and bilinear constraints in Equations (6) and (7) are non-convex. Thus, we reformulate *PS1* into a convex model, shown as follows.

We rewrite Equations (6) and (7):

$$t^H_{i,j,k} = \hat{T}^H_{i,k} - \frac{\hat{q}_{i,j,k}}{f^H_{i,j,k}} \qquad \forall i \in HP, j \in CP, k \in ST, \hat{z}_{i,j,k} = 1, Y^H_{i,k} = 1 \tag{15}$$

$$t^C_{i,j,k} = \hat{T}^C_{j,k+1} + \frac{\hat{q}_{i,j,k}}{f^C_{i,j,k}} \qquad \forall i \in HP, j \in CP, k \in ST, \hat{z}_{i,j,k} = 1, Y^C_{j,k} = 1 \tag{16}$$

Substituting $t^H_{i,j,k}$ and $t^C_{i,j,k}$ by their expressions in Equations (15) and (16) and also substituting the areas ($A_{i,j,k}$), we obtain the following problem namely *PS2*.

$$\begin{aligned} Min \Bigg\{ & \sum_{\substack{i\in HP \\ Y^H_{i,k}=1}} \sum_{\substack{j\in CP \\ Y^C_{j,k}=1}} \sum_{\substack{k\in ST \\ \hat{z}_{i,j,k}=1}} \left\{ \frac{\hat{q}_{i,j,k}\,\widehat{U}^{-1}_{ij}}{\left[\frac{2}{3}\sqrt{\left(\hat{T}^H_{i,k} - \hat{T}^C_{j,k+1} - \frac{\hat{q}_{i,j,k}}{f^H_{i,j,k}}\right)\left(\hat{T}^H_{i,k} - \hat{T}^C_{j,k+1} - \frac{\hat{q}_{i,j,k}}{f^C_{i,j,k}}\right)} + \frac{1}{6}\left(\hat{T}^H_{i,k} - \hat{T}^C_{j,k+1} - \frac{\hat{q}_{i,j,k}}{f^H_{i,j,k}}\right) + \frac{1}{6}\left(\hat{T}^H_{i,k} - \hat{T}^C_{j,k+1} - \frac{\hat{q}_{i,j,k}}{f^C_{i,j,k}}\right) \right]} \right\}^{\hat{c}} \\ & + \sum_{\substack{i\in HP \\ Y^H_{i,k}=1}} \sum_{\substack{j\in CP \\ Y^C_{j,k}=0}} \sum_{\substack{k\in ST \\ \hat{z}_{i,j,k}=1}} \left\{ \frac{\hat{q}_{i,j,k}\,\widehat{U}^{-1}_{ij}}{\left[\frac{2}{3}\sqrt{\left(\hat{T}^H_{i,k} - \hat{T}^C_{j,k}\right)\left(\hat{T}^H_{i,k} - \hat{T}^C_{j,k+1} - \frac{\hat{q}_{i,j,k}}{f^H_{i,j,k}}\right)} + \frac{1}{6}\left(\hat{T}^H_{i,k} - \hat{T}^C_{j,k}\right) + \frac{1}{6}\left(\hat{T}^H_{i,k} - \hat{T}^C_{j,k+1} - \frac{\hat{q}_{i,j,k}}{f^H_{i,j,k}}\right) \right]} \right\}^{\hat{c}} \\ & + \sum_{\substack{i\in HP \\ Y^H_{i,k}=0}} \sum_{\substack{j\in CP \\ Y^C_{j,k}=1}} \sum_{\substack{k\in ST \\ \hat{z}_{i,j,k}=1}} \left\{ \frac{\hat{q}_{i,j,k}\,\widehat{U}^{-1}_{ij}}{\left[\frac{2}{3}\sqrt{\left(\hat{T}^H_{i,k+1} - \hat{T}^C_{j,k+1}\right)\left(\hat{T}^H_{i,k} - \hat{T}^C_{j,k+1} - \frac{\hat{q}_{i,j,k}}{f^C_{i,j,k}}\right)} + \frac{1}{6}\left(\hat{T}^H_{i,k+1} - \hat{T}^C_{j,k+1}\right) + \frac{1}{6}\left(\hat{T}^H_{i,k} - \hat{T}^C_{j,k+1} - \frac{\hat{q}_{i,j,k}}{f^C_{i,j,k}}\right) \right]} \right\}^{\hat{c}} \Bigg\} \end{aligned} \tag{17}$$

$$\sum_{j \in CP, \widehat{z}_{i,j,k}=1} f^H_{i,j,k} - Fcp^H_i = 0 \qquad \forall i \in HP, k \in ST, Y^H_{i,k} = 1 \tag{18}$$

$$\sum_{i \in HP, \widehat{z}_{i,j,k}=1} f^C_{i,j,k} - Fcp^C_j = 0 \qquad \forall j \in CP, k \in ST, Y^C_{j,k} = 1 \tag{19}$$

$$\begin{aligned} &\widehat{q}_{i,j,k} + f^H_{i,j,k}\left(\widehat{T}^C_{j,k+1} - \widehat{T}^H_{i,k} + \mathrm{EMAT_{Min}}\right) \le 0 \\ &\forall i \in HP, j \in CP, k \in ST, \widehat{z}_{i,j,k} = 1, Y^H_{i,k} = 1 \end{aligned} \tag{20}$$

$$\begin{aligned} &\widehat{q}_{i,j,k} + f^C_{i,j,k}\left(\widehat{T}^C_{j,k+1} - \widehat{T}^H_{i,k} + \mathrm{EMAT_{Min}}\right) \le 0 \\ &\forall i \in HP, j \in CP, k \in ST, \widehat{z}_{i,j,k} = 1, Y^C_{j,k} = 1 \end{aligned} \tag{21}$$

The objective function of *PS2* is a sum of convex terms. Indeed, the terms are the inverse of LMTD function elevated to a constant $\widehat{c}$. We recognize LMTD is concave as proven by Mistry and Misener.[23] Even if we use an approximation, this continues to be true. In Supporting Information-Part C, we provide the proof that the objective function of *PS2* is convex. In turn, the system of equations corresponding to the KKT condition of *PS2* that we solve in Strategy 3 is given in Supporting Information-Part D. Because the problem is convex, one can just solve this system of equations and obtain the optimum. While it is known that solving these equations directly for large-scale systems may exhibit difficulties, we have not observed them in our work.

4 | ENERGY BOUND MODELS

Before performing the Golden Search for a minimal or non-minimal network, it is necessary to obtain the bounds of energy consumption (total hot utility demand) E^{Niso}_{Min} and E^{Niso}_{Max}. For non-isothermal mixing, E^{Niso}_{Min} and E^{Niso}_{Max} are in general different from E^{Iso}_{Min} and E^{Iso}_{Max} (isothermal mixing). For this, we develop models namely PE^{Niso}_{Min} and PE^{Niso}_{Max} to obtain E^{Niso}_{Min} and E^{Niso}_{Max}, respectively. The formulation of PE^{Niso}_{Min} is the following:

$$PE^{Niso}_{Min} = \underset{\forall (T,Q) \in D_{Synheat}}{Min} \; E \tag{22}$$

$$E = \sum_{j \in CP, \widehat{zhu}_j=1} qhu_j \tag{23}$$

$$\sum_{j \in CP, \widehat{z}_{i,j,k}=1} f^H_{i,j,k} - Fcp^H_i = 0 \qquad \forall i \in HP, k \in ST, Y^H_{i,k} = 1 \tag{24}$$

$$\sum_{i \in HP, \widehat{z}_{i,j,k}=1} f^C_{i,j,k} - Fcp^C_j = 0 \qquad \forall j \in CP, k \in ST, Y^C_{j,k} = 1 \tag{25}$$

$$\Delta t^C_{i,j,k} = \left(T^H_{i,k} - \frac{q_{i,j,k}}{f^H_{i,j,k}}\right) - T^C_{j,k+1} \qquad \forall i \in HP, j \in CP, k \in ST, \widehat{z}_{i,j,k} = 1, Y^H_{i,k} = 1 \tag{26}$$

$$\Delta t^H_{i,j,k} = T^H_{i,k} - \left(T^C_{j,k+1} + \frac{q_{i,j,k}}{f^C_{i,j,k}}\right) \qquad \forall i \in HP, j \in CP, k \in ST, \widehat{z}_{i,j,k} = 1, Y^C_{j,k} = 1 \tag{27}$$

$$\Delta t^C_{i,j,k} = T^H_{i,k+1} - T^C_{j,k+1} \qquad \forall i \in HP, j \in CP, k \in ST, \widehat{z}_{i,j,k} = 1, Y^H_{i,k} = 0 \tag{28}$$

$$\Delta t^H_{i,j,k} = T^H_{i,k} - T^C_{j,k} \qquad \forall i \in HP, j \in CP, k \in ST, \widehat{z}_{i,j,k} = 1, Y^C_{j,k} = 0 \tag{29}$$

$$\Delta thu_j = Thu^{out} - T^C_{j,1} \qquad \forall j \in CP, \widehat{z}hu_j = 1 \tag{30}$$

$$\Delta tcu_i = T^H_{i,K} - Tcu^{out} \qquad \forall i \in HP, \widehat{z}cu_i = 1 \tag{31}$$

$$\Delta t^C_{i,j,k} \ge EMAT_{Min} \qquad \forall i \in HP, j \in CP, k \in ST, \widehat{z}_{i,j,k} = 1 \tag{32}$$

$$\Delta t^H_{i,j,k} \ge EMAT_{Min} \qquad \forall i \in HP, j \in CP, k \in ST, \widehat{z}_{i,j,k} = 1 \tag{33}$$

$$\Delta thu_j \ge EMAT_{Min} \qquad \forall j \in CP, \widehat{z}hu_j = 1 \tag{34}$$

$$\Delta tcu_i \ge EMAT_{Min} \qquad \forall i \in HP, \widehat{z}cu_i = 1 \tag{35}$$

It should be noted that the variables qhu_j do not participate/present explicitly in any other equations in this model. However, they are implicit in $D_{Synheat}$ (Synheat).

The formulation of PE^{Niso}_{Max} includes the same constraints of PE^{Niso}_{Min}(Equations (24)–(35)), but the objective function is:

$$PE^{Niso}_{Max} = \underset{\forall (T,Q) \in D_{Synheat}}{Max} \; E \tag{36}$$

The above two models are both non-convex problems and can be solved using a global solver. However, we solve a system of equations (named Sy_E) and propose two sub-algorithms, namely PBE_{Min} and PBE_{Max}, to obtain the minimum and maximum energy, respectively. The system of equations Sy_E is composed of the constraints of PE^{Niso}_{Min} (Equations (24)–(35)) associated to the substitution of the variable E in Equation (23) by a fixed parameter ($\widehat{E}$):

$$\widehat{E} = \sum_{j \in CP, \widehat{zhu}_j=1} qhu_j \tag{37}$$

The sub-algorithm PBE_{Min} includes the following steps (the corresponding flowchart is shown in Supporting Information-Part E).

1. Start from $E^{Lo}_{Min} = E^{User}_{Min}$.
2. Run PE_{Min} to obtain E^{Iso}_{Min} and set $E^{Up}_{Min} = E^{Iso}_{Min}$.
3. If $\frac{E^{Up}_{Min} - E^{Lo}_{Min}}{E^{Up}_{Min}} < \widehat{\varepsilon}$, go to Step 6. Otherwise, go to next step.
4. Solve Sy_E for $\widehat{E} = E^{Lo}_{Min}$. If feasible, $E^{Up}_{Min} = E^{Lo}_{Min}$ and go to Step 6. Otherwise, go to next step.
5. Solve Sy_E for $\widehat{E} = \frac{E^{Up}_{Min} + E^{Lo}_{Min}}{2}$. If feasible, $E^{Up}_{Min} = \frac{E^{Up}_{Min} + E^{Lo}_{Min}}{2}$. Otherwise, $E^{Lo}_{Min} = \frac{E^{Up}_{Min} + E^{Lo}_{Min}}{2}$. Then, go to Step 3.
6. $E^{Niso}_{Min} = E^{Up}_{Min}$ and stop.

The sub-algorithm PBE_{Max} includes the following steps (the corresponding flowchart is shown in Supporting Information-Part E).

1. Start from $E_{Max}^{Up} = E_{Max}^{User}$.
2. Run PE_{Max} to obtain E_{Max}^{Iso} and set $E_{Max}^{Lo} = E_{Max}^{Iso}$.
3. If $\frac{E_{Max}^{Up} - E_{Max}^{Lo}}{E_{Max}^{Up}} < \widehat{\varepsilon}$, go to Step 6. Otherwise, go to next step.
4. Solve Sy_E for $\widehat{E} = E_{Max}^{Up}$. If feasible, $E_{Max}^{Lo} = E_{Max}^{Up}$ and go to Step 6. Otherwise, go to next step.
5. Solve Sy_E for $\widehat{E} = \frac{E_{Max}^{Up} + E_{Max}^{Lo}}{2}$. If feasible, $E_{Max}^{Lo} = \frac{E_{Max}^{Up} + E_{Max}^{Lo}}{2}$. Otherwise, $E_{Max}^{Up} = \frac{E_{Max}^{Up} + E_{Max}^{Lo}}{2}$. Then, go to Step 3.
6. $E_{Max}^{Niso} = E_{Max}^{Lo}$ and stop.

5 | BINDING EMAT LOCATION MODELS

In Part II, two models, namely *PLOC1* and *PLOC*, are used to find the EMAT-binding location of energy loop for non-MSTR network. We now present a new version of *PLOC1* namely *PLOC1S* that includes Equations (24)–(35) and the following ones:

$$\beta \geq EMAT_{Min} \tag{38}$$

$$\beta \leq \Delta t_{i,j,k}^{H} \qquad \forall i \in HP, j \in CP, k \in ST, \widehat{z}_{i,j,k} = 1 \tag{39}$$

$$\beta \leq \Delta t_{i,j,k}^{C} \qquad \forall i \in HP, j \in CP, k \in ST, \widehat{z}_{i,j,k} = 1 \tag{40}$$

$$\beta \leq \Delta thu_j \qquad \forall j \in CP, \widehat{zhu}_j = 1 \tag{41}$$

$$\beta \leq \Delta tcu_i \qquad \forall i \in HP, \widehat{zcu}_i = 1 \tag{42}$$

$$\left(\Delta t_{i,j,k}^{H} - \beta\right) + \left(1 - y_{i,j,k}^{H}\right) \Gamma_{i,j} \geq 0 \qquad \forall i \in HP, j \in CP, k \in ST, \widehat{z}_{i,j,k} = 1 \tag{43}$$

$$\left(\Delta t_{i,j,k}^{H} - \beta\right) + \left(y_{i,j,k}^{H} - 1\right) \Gamma_{i,j} \leq 0 \qquad \forall i \in HP, j \in CP, k \in ST, \widehat{z}_{i,j,k} = 1 \tag{44}$$

$$\left(\Delta t_{i,j,k}^{C} - \beta\right) + \left(1 - y_{i,j,k}^{C}\right) \Gamma_{i,j} \geq 0 \qquad \forall i \in HP, j \in CP, k \in ST, \widehat{z}_{i,j,k} = 1 \tag{45}$$

$$\left(\Delta t_{i,j,k}^{C} - \beta\right) + \left(y_{i,j,k}^{C} - 1\right) \Gamma_{i,j} \leq 0 \qquad \forall i \in HP, j \in CP, k \in ST, \widehat{z}_{i,j,k} = 1 \tag{46}$$

$$\left(\Delta thu_j - \beta\right) + \left(1 - yhu_j\right) \Gamma_j \geq 0 \qquad \forall j \in CP, \widehat{zhu}_j = 1 \tag{47}$$

$$\left(\Delta thu_j - \beta\right) + \left(yhu_j - 1\right) \Gamma_j \leq 0 \qquad \forall j \in CP, \widehat{zhu}_j = 1 \tag{48}$$

$$\left(\Delta tcu_i - \beta\right) + \left(1 - ycu_i\right) \Gamma_i \geq 0 \qquad \forall i \in HP, \widehat{zcu}_i = 1 \tag{49}$$

$$\left(\Delta tcu_i - \beta\right) + \left(ycu_i - 1\right) \Gamma_i \leq 0 \qquad \forall i \in HP, \widehat{zcu}_i = 1 \tag{50}$$

$$\sum_{i \in HP} \sum_{j \in CP} \sum_{k \in ST, \widehat{z}_{i,j,k} = 1,} \left(y_{i,j,k}^{H} + y_{i,j,k}^{C}\right) + \sum_{\widehat{zhu}_j = 1} yhu_j + \sum_{\widehat{zcu}_i = 1} ycu_i \geq 1 \tag{51}$$

Once *PLOC1S* is solved, the value of energy consumption (E^*), heat loads of heat exchangers ($q_{i,j,k}^*$, qhu_j^*, and qcu_i^*) as well as the values of $y_{i,j,k}^{H*}$, $y_{i,j,k}^{C*}$, yhu_j^*, and ycu_i^* that represent the potential EMAT-binding location are obtained.

In turn, model *PLOC* is revised as the one namely *PLOCS* that is the system of equations including Equations (24)–(35) and the following ones:

$$\sum_{j \in CP, \widehat{zhu}_j = 1} qhu_j = E^* \tag{52}$$

$$q_{i,j,k} = q_{i,j,k}^* - \widehat{\Delta} \qquad \forall i \in HP, j \in CP, k \in ST, \widehat{z}_{i,j,k} = 1, y_{i,j,k}^{H*} = 1 \vee y_{i,j,k}^{C*} = 1 \tag{53}$$

$$qhu_j = qhu_j^* - \widehat{\Delta} \qquad \forall j \in CP, \widehat{zhu}_j = 1, yhu_j^* = 1 \tag{54}$$

$$qcu_i = qcu_i^* - \widehat{\Delta} \qquad \forall i \in HP, \widehat{zcu}_i = 1, ycu_i^* = 1 \tag{55}$$

If *PLOCS* is feasible, the energy loop, represented by the binary parameters $y_{i,j,k}^{H*}$, $y_{i,j,k}^{C*}$, yhu_j^*, and ycu_i^*, is found. Otherwise, the location does not belong to the energy loop. Then, we exclude this location to find another potential one by running *PLOC1S* again. In a word, *PLOC1S* and *PLOCS* are run recursively until the former is infeasible.

6 | BINDING EMAT BOUNDS MODELS

For non-minimal networks with fixed energy consumption, it is necessary to obtain the lower and upper bounds ($\widehat{EMAT}_{Min}$ and $\widehat{EMAT}_{Max}$) of the binding EMAT with the fixed location. For this purpose, we develop two models namely $PEMAT_{Min}^{Niso}$ and $PEMAT_{Max}^{Niso}$ shown as follows.

The formulation of $PEMAT_{Min}^{Niso}$ includes Equations (24)–(35) and the following ones:

$$PEMAT_{Min}^{Niso} = \underset{\forall (T,Q) \in D_{Synheat}}{Min} EMAT \tag{56}$$

$$\sum_{j \in CP, \widehat{zhu}_j} qhu_j = \widehat{E} \tag{57}$$

$$\left(\Delta t_{i,j,k}^{H} - EMAT\right) + \left(1 - y_{i,j,k}^{H*}\right) \Gamma_{i,j} \geq 0 \qquad \forall i \in HP, j \in CP, k \in ST, \widehat{z}_{i,j,k} = 1 \tag{58}$$

$$\left(\Delta t_{i,j,k}^{H} - EMAT\right) + \left(y_{i,j,k}^{H*} - 1\right) \Gamma_{i,j} \leq 0 \qquad \forall i \in HP, j \in CP, k \in ST, \widehat{z}_{i,j,k} = 1 \tag{59}$$

$$\left(\Delta t_{i,j,k}^{C} - EMAT\right) + \left(1 - y_{i,j,k}^{C*}\right) \Gamma_{i,j} \geq 0 \qquad \forall i \in HP, j \in CP, k \in ST, \widehat{z}_{i,j,k} = 1 \tag{60}$$

$$\left(\Delta t^{C}_{i,j,k} - EMAT\right) + \left(y^{C*}_{i,j,k} - 1\right) \Gamma_{i,j} \le 0 \quad \forall i \in HP, j \in CP, k \in ST, \widehat{z}_{i,j,k} = 1 \tag{61}$$

$$\left(\Delta thu_j - EMAT\right) + \left(1 - yhu^*_j\right) \Gamma_j \ge 0 \quad \forall j \in CP, \widehat{z}hu_j = 1 \tag{62}$$

$$\left(\Delta thu_j - EMAT\right) + \left(yhu^*_j - 1\right) \Gamma_j \le 0 \quad \forall j \in CP, \widehat{z}hu_j = 1 \tag{63}$$

$$\left(\Delta tcu_i - EMAT\right) + \left(1 - ycu^*_i\right) \Gamma_i \ge 0 \quad \forall i \in HP, \widehat{z}cu_i = 1 \tag{64}$$

$$\left(\Delta tcu_i - EMAT\right) + \left(ycu^*_i - 1\right) \Gamma_i \le 0 \quad \forall i \in HP, \widehat{z}cu_i = 1 \tag{65}$$

The formulation of $PEMAT^{Niso}_{Max}$ is composed of the same constraints of $PEMAT^{Niso}_{Min}$ associated to the following objective function:

$$PEMAT^{Niso}_{Max} = \underset{\forall (T,Q) \in D_{Synheat}}{Max} \; EMAT \tag{66}$$

The above NLMs $PEMAT^{Niso}_{Min}$ and $PEMAT^{Niso}_{Max}$ can be solved using a global solver. Instead, however, we solve the following system of equations namely Sy_{EMAT} and develop two sub-algorithms namely $PBEMAT_{Min}$ and $PBEMAT_{Max}$ to obtain the minimum and maximum bounds of binding EMAT, respectively. The system of equations Sy_{EMAT} corresponds to the constraints of $PEMAT^{Niso}_{Min}$ but Equations (58)–(65) are replaced by the following ones:

$$\left(\Delta t^{H}_{i,j,k} - \widehat{E}MAT\right) + \left(1 - y^{H*}_{i,j,k}\right) \Gamma_{i,j} \ge 0 \quad \forall i \in HP, j \in CP, k \in ST, \widehat{z}_{i,j,k} = 1 \tag{67}$$

$$\left(\Delta t^{H}_{i,j,k} - \widehat{E}MAT\right) + \left(y^{H*}_{i,j,k} - 1\right) \Gamma_{i,j} \le 0 \quad \forall i \in HP, j \in CP, k \in ST, \widehat{z}_{i,j,k} = 1 \tag{68}$$

$$\left(\Delta t^{C}_{i,j,k} - \widehat{E}MAT\right) + \left(1 - y^{C*}_{i,j,k}\right) \Gamma_{i,j} \ge 0 \quad \forall i \in HP, j \in CP, k \in ST, \widehat{z}_{i,j,k} = 1 \tag{69}$$

$$\left(\Delta t^{C}_{i,j,k} - \widehat{E}MAT\right) + \left(y^{C*}_{i,j,k} - 1\right) \Gamma_{i,j} \le 0 \quad \forall i \in HP, j \in CP, k \in ST, \widehat{z}_{i,j,k} = 1 \tag{70}$$

$$\left(\Delta thu_j - \widehat{E}MAT\right) + \left(1 - yhu^*_j\right) \Gamma_j \ge 0 \quad \forall j \in CP, \widehat{z}hu_j = 1 \tag{71}$$

$$\left(\Delta thu_j - \widehat{E}MAT\right) + \left(yhu^*_j - 1\right) \Gamma_j \le 0 \quad \forall j \in CP, \widehat{z}hu_j = 1 \tag{72}$$

$$\left(\Delta tcu_i - \widehat{E}MAT\right) + \left(1 - ycu^*_i\right) \Gamma_i \ge 0 \quad \forall i \in HP, \widehat{z}cu_i = 1 \tag{73}$$

$$\left(\Delta tcu_i - \widehat{E}MAT\right) + \left(ycu^*_i - 1\right) \Gamma_i \le 0 \quad \forall i \in HP, \widehat{z}cu_i = 1 \tag{74}$$

The sub-algorithm $PBEMAT_{Min}$ includes the following steps (the corresponding flowchart is shown in Supporting Information-Part E).

1. Start from $\widehat{E}MAT^{Lo}_{Min} = EMAT_{Min}$.
2. Run $PEMAT^{Iso}_{Min}$ to obtain $\widehat{E}MAT^{Up}_{Min}$ and set $\widehat{E}MAT^{Up}_{Min} = \widehat{E}MAT^{Iso}_{Min}$.
3. If $\frac{\widehat{EMAT}^{Up}_{Min} - \widehat{EMAT}^{Lo}_{Min}}{\widehat{EMAT}^{Up}_{Min}} < \widehat{\varepsilon}$, go to Step 6. Otherwise, go to the next step.
4. Solve Sy_{EMAT} for $\widehat{E}MAT = \widehat{E}MAT^{Lo}_{Min}$. If feasible, $\widehat{E}MAT^{Up}_{Min} = \widehat{E}MAT^{Lo}_{Min}$ and go to Step 6. Otherwise, go to the next step.
5. Solve Sy_{EMAT} for $\widehat{E}MAT = \frac{\widehat{EMAT}^{Up}_{Min} + \widehat{EMAT}^{Lo}_{Min}}{2}$. If feasible, $\widehat{E}MAT^{Up}_{Min} = \frac{\widehat{EMAT}^{Up}_{Min} + \widehat{EMAT}^{Lo}_{Min}}{2}$. Otherwise, $\widehat{E}MAT^{Lo}_{Min} = \frac{\widehat{EMAT}^{Up}_{Min} + \widehat{EMAT}^{Lo}_{Min}}{2}$. Then, go to Step 3.
6. $\widehat{E}MAT_{Min} = \widehat{E}MAT^{Up}_{Min}$ and stop.

The sub-algorithm $PBEMAT_{Max}$ includes the following steps (the corresponding flowchart is shown in Supporting Information-Part E).

1. Start from $\widehat{E}MAT^{Up}_{Max} = HRAT^{User}_{Max}$.
2. Run $PEMAT^{Iso}_{Max}$ to obtain $\widehat{E}MAT^{Lo}_{Max}$ and set $\widehat{E}MAT^{Lo}_{Max} = \widehat{E}MAT^{Iso}_{Max}$.
3. If $\frac{\widehat{EMAT}^{Up}_{Max} - \widehat{EMAT}^{Lo}_{Max}}{\widehat{EMAT}^{Up}_{Max}} < \widehat{\varepsilon}$, go to Step 6. Otherwise, go to the next step.
4. Solve Sy_{EMAT} for $\widehat{E}MAT = \widehat{E}MAT^{Up}_{Max}$. If feasible, $\widehat{E}MAT^{Lo}_{Max} = \widehat{E}MAT^{Up}_{Max}$ and go to Step 6. Otherwise, go to the next step.
5. Solve Sy_{EMAT} for $\widehat{E}MAT = \frac{\widehat{EMAT}^{Up}_{Max} + \widehat{EMAT}^{Lo}_{Max}}{2}$. If feasible, $\widehat{E}MAT^{Lo}_{Max} = \frac{\widehat{EMAT}^{Up}_{Max} + \widehat{EMAT}^{Lo}_{Max}}{2}$. Otherwise, $\widehat{E}MAT^{Up}_{Max} = \frac{\widehat{EMAT}^{Up}_{Max} + \widehat{EMAT}^{Lo}_{Max}}{2}$. Then, go to Step 3.
6. $\widehat{E}MAT_{Max} = \widehat{E}MAT^{Lo}_{Max}$ and stop.

7 | GLOBAL OPTIMUM SEARCH ALGORITHM

Based on the above models and sub-algorithms, we develop a new Global Optimum Search Algorithm. Figure 3 depicts the flowchart of this algorithm that includes the following steps.

1. The Synheat model (see Appendix A of Part I) is run without the area costs to minimize the number of heat exchangers (N_{min}) with the given energy bounds $\widehat{E}^{User}_{Min}$ and $\widehat{E}^{User}_{Max}$. This step is exactly the same as the one in Parts I and II, and the models involved were presented there. Also, set $N = N_{min}$ and start by giving a large value to the incumbent TAC namely $UBTAC = +\infty$. Go to the next step.
2. For current N, run one of the following two options.
   - Option 1: Run *PLB* to enumerate a structure.
   - Option 2: Run *PSTR* to enumerate a structure.

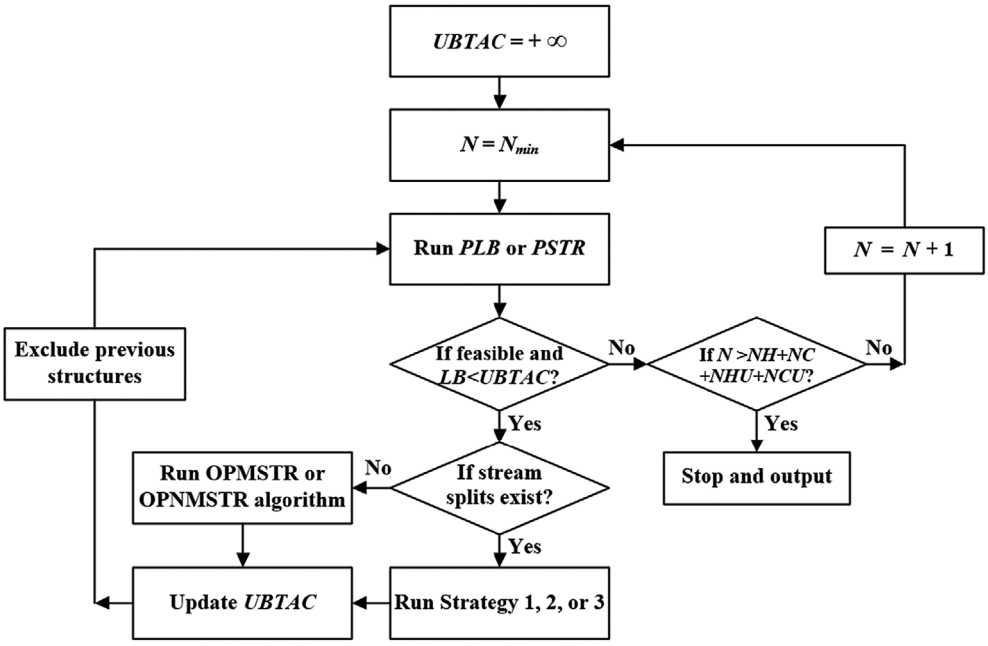

FIGURE 3 Flowchart of the proposed Global Optimum Search Algorithm

3. If the chosen strategy is not Strategy 1, go to the next step. Otherwise, solve the resulting NLP using a global solver (e.g. BARON) for the considered structure to obtain the cost TAC_{STR} and then go to Step 5.
4. For the considered structure, obtain the values of $Y^H_{i,k}$ and $Y^C_{j,k}$ to ascertain if there is a stream split.
   - If there is no split, use the appropriate Golden Search-based algorithms from Parts I and II to obtain the cost TAC_{STR}.
   - If there is a split, incorporate the split flows optimization steps outlined above to obtain the cost TAC_{STR} using Strategy 2 or Strategy 3 when obtaining the *TAC* for each value of the energy consumption and the binding *EMAT*.

   Then, go to next step.
5. Update *UBTAC*: If $TAC_{STR} < UBTAC$, $UBTAC = TAC_{STR}$. Go to the next step.
6. Exclude previously found structures by running one of the following options.
   - Option 1: run *PLBR* to enumerate another structure. If it is feasible and $RTAC \leq UBTAC$, go to Step 3. Otherwise, if infeasible or if feasible but $RTAC > UBTAC$, go to Step 7.
   - Option 2: run *PSTRR* to enumerate another structure. If feasible, go to Step 3. Otherwise, go to Step 7.
7. If $N > NH + NC + NHU + NCU$, output *UBTAC* and stop. Otherwise, increase the total number of heat exchangers by $N = N + 1$ and go to Step 2.

8 | EXAMPLES

Nineteen problems of different sizes, which include Examples 1–16 tested in Parts I and II as well as three additional examples, are solved for illustration purposes. All examples are implemented in GAMS (version 23.7)[34] on a PC machine (i7 3.6 GHz, 8 GB RAM). The solution results are presented in Table 1 that also includes the solution results in Part II for comparison purposes. The total number of the HEN structures enumerated is the same as the one in Part II, and only TACs and solution time are listed and compared. The solution times for our Strategies 1–3, proposed in this work, are presented in Table 2.

Table 1 shows the TACs of Examples 2, 5, 6, 16, 17, 18, and 19 are reduced by 1.2%–8.6% when considering non-isothermal mixing. Meanwhile, the TACs of Examples 1 and 3 are the same as the ones in our Part II, because no stream splits exist in the optimal structures. The TACs of Examples 4, 7, 8, 9, 10, 11, 12, 13, 14, and 15 decrease slightly ($\leq$ 1.0%), showing that the optimal solutions of isothermal and non-isothermal mixing are very closed in these problems. Table 1 also shows that in Examples 1–7 our Option 1 (*PLB*, smart enumeration using LB model) is faster than Option 2 (*PSTR*, exhaustive enumeration). This is mainly because Examples 1–7 are not large-scale problems and the lower bound (*PLB*) model in Option 1 can update the lower bounds effectively. On the contrary, for Examples 8–16, Option 2 (*PSTR*) is faster, since these problems are large-scale cases. This observation illustrates that when example size increases, the solution time becomes longer and the option using the lower bound (*PLB*) model is not viable unless this smart search is paralleled. It should be pointed out that we have tried to use a different number of intervals to construct the lower bound (*PLB*) model, for instance, 2, 5, 8, 10, 20, 30, 40, 50, 60, 70, 80, etc. Then, we pick the number of intervals that renders the minimum solution time. Future research will explore new ways to decrease the solution time. All the solution results of examples are compared with the ones from Part II and the literature solutions in Supporting Information-Part F.

Regarding strategies, Table 2 indicates that in Examples 1–4 our Strategy 1 using the global solver BARON is faster than Strategies 2 and 3. This obversion illustrates that BARON can globally and

TABLE 1 Solution comparison of Examples 1–19

	Solutions in Part II				Solutions in this work (Part III)			
	PLB		*PSTR*		*PLB*		*PSTR*	
Example	TAC ($/year)	Time (s)	TAC ($/year)	Time (s)	TAC ($/year)	Time (s)	TAC ($/year)	Time (s)
1 (2H, 2C)[22]	154,910.6	90.0	154,910.6	168.9	154,910.6	239.1	154,910.6	398.2
2 (2H, 2C)[35]	360,037.2	36.5	360,037.2	162.3	355,701.5	139.5	355,701.5	512.1
3 (2H, 2C)[36]	715,962.9	69.1	715,962.9	196.2	715,962.9	129.2	715,962.9	306.5
4 (3H, 2C)[21]	80,959.6	15.2	80,959.6	369.2	80,847.7	63.2	80,847.7	539.6
5 (3H, 2C)[30]	1,758,381.0	125.6	1,758,381.0	598.2	1,731,819.6	226.8	1,731,819.6	972.5
6 (5H, 1C)[23]	632,360.7	122.3	632,360.7	398.5	624,569.1	239.3	624,569.1	681.3
7 (3H, 4C)[37]	177,261.3	652.3	177,261.3	1932.5	176,097.1	922.7	176,097.1	2833.5
8 (5H, 5C)[38]	-	>360,000	64,015.0	31,502.8	-	>360,000	64015.0	48,335.9
9 (5H, 5C)[39]	-	>360,000	109,078.4	25,659.3	-	>360,000	109,078.4	39,218.8
10 (5H, 5C)[26]	-	>360,000	43,329.2	31,235.8	-	>360,000	43,314.0	53,625.7
11 (11H, 2C)[30]	-	>360,000	3,441,663.0	55,689.3	-	>360,000	3,424,958.8	79,336.5
12 (6H, 5C)[12]	-	>360,000	139,398.1	69,623.8	-	>360,000	139,387.0	82,559.3
13 (6H, 10C)[40]	-	>360,000	6,674,677.0	80,715.9	-	>360,000	6,654,330.1	109,336.8
14 (8H, 7C)[12]	-	>360,000	1,501,004.0	89,625.9	-	>360,000	1,498,935.1	112,758.3
15 (13H, 7C)[41]	-	>360,000	1,414,857.0	100,568.8	-	>360,000	1,407,203.3	183,682.1
16 (22H, 17C)[12]	-	>360,000	1,912,763.0	183,286.5	-	>360,000	1,840,936.2	332,693.6
17 (1H, 2C)[28]	52,430.9	16.8	52,430.9	30.2	48,663.3	56.5	48,663.3	79.3
18 (3H, 2C)[28]	100,770.2	95.9	100,770.2	256.1	95,661.1	199.3	95,661.1	332.5
19 (2H, 4C)[20]	140,367.1	369.8	140,367.1	692.3	128,236.7	589.2	128,236.7	962.5

TABLE 2 Solution times (s) of Strategies 1–3

	Option 1 (*PLB*)			Option 2 (*PSTR*)		
Example	Strategy 1	Strategy 2	Strategy 3	Strategy 1	Strategy 2	Strategy 3
1 (2H, 2C)[22]	239.1	380.5	312.6	398.2	502.7	462.6
2 (2H, 2C)[35]	139.5	305.6	236.7	512.1	711.5	620.3
3 (2H, 2C)[36]	129.2	291.3	212.5	306.5	511.3	409.8
4 (3H, 2C)[21]	63.2	101.3	85.3	539.6	737.2	655.2
5 (3H, 2C)[30]	521.6	303.9	226.8	1321.2	1135.6	972.5
6 (5H, 1C)[23]	532.8	318.2	239.3	825.3	765.2	681.3
7 (3H, 4C)[37]	2391.5	1235.9	922.7	3952.8	3361.7	2833.5
8 (5H, 5C)[38]	>360,000	>360,000	>360,000	68,332.5	52,661.7	48,335.9
9 (5H, 5C)[39]	>360,000	>360,000	>360,000	56,335.6	43,205.3	39,218.8
10 (5H, 5C)[26]	>360,000	>360,000	>360,000	68,329.8	59,337.6	53,625.7
11 (11H, 2C)[30]	>360,000	>360,000	>360,000	>360,000	83,329.6	79,336.5
12 (6H, 5C)[12]	>360,000	>360,000	>360,000	>360,000	90,625.8	82,559.3
13 (6H, 10C)[40]	>360,000	>360,000	>360,000	>360,000	113,552.9	109,336.8
14 (8H, 7C)[12]	>360,000	>360,000	>360,000	>360,000	136,621.2	112,758.3
15 (13H, 7C)[41]	>360,000	>360,000	>360,000	>360,000	212,335.6	183,682.1
16 (22H, 17C)[12]	>360,000	>360,000	>360,000	>360,000	379,652.8	332,693.6
17 (1H, 2C)[28]	56.5	72.2	63.5	79.3	95.8	86.2
18 (3H, 2C)[28]	199.3	239.2	212.7	332.5	452.5	401.9
19 (2H, 4C)[20]	792.5	682.5	589.2	1569.1	1322.8	962.5

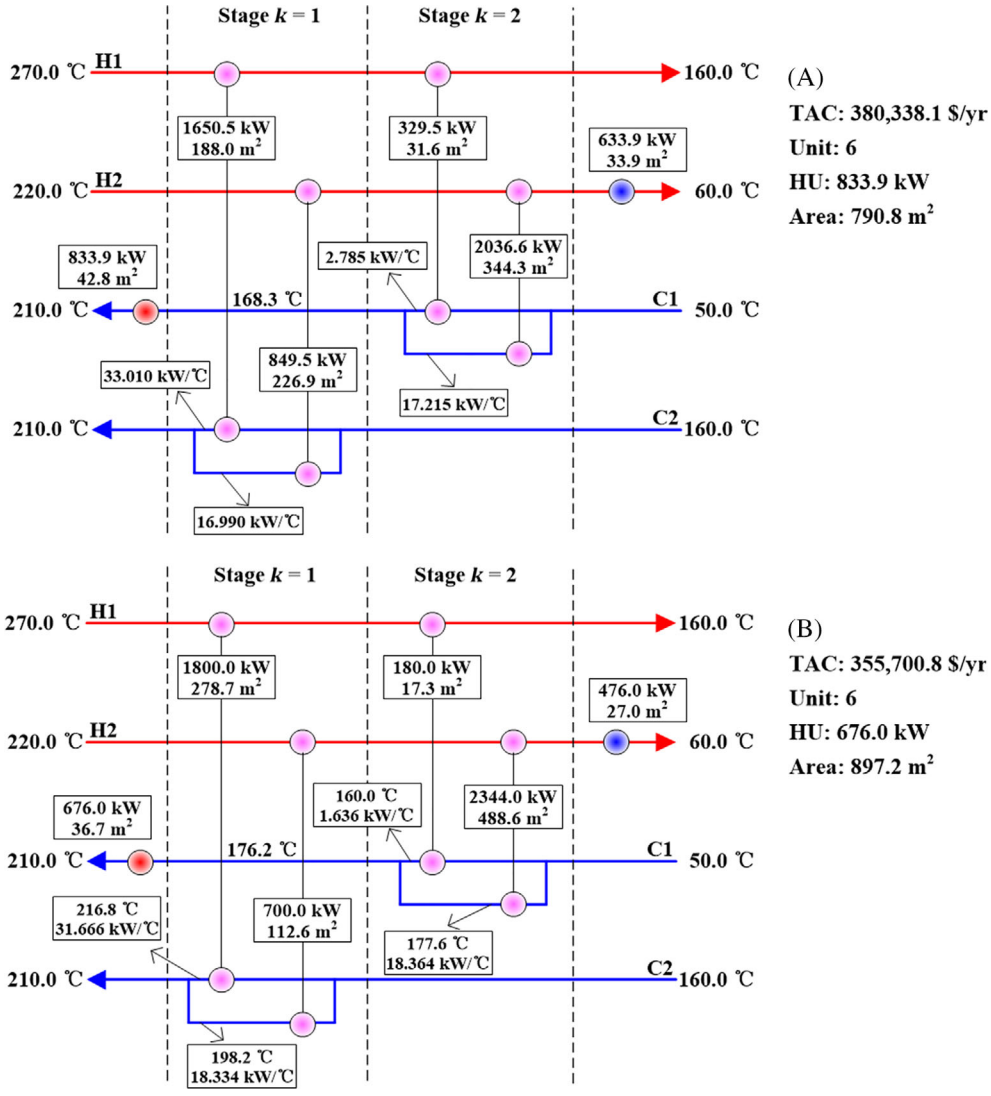

FIGURE 4 The flowsheets for the optimal structure of Example 2: (A) HEN with isothermal mixing and (B) HEN with non-isothermal mixing

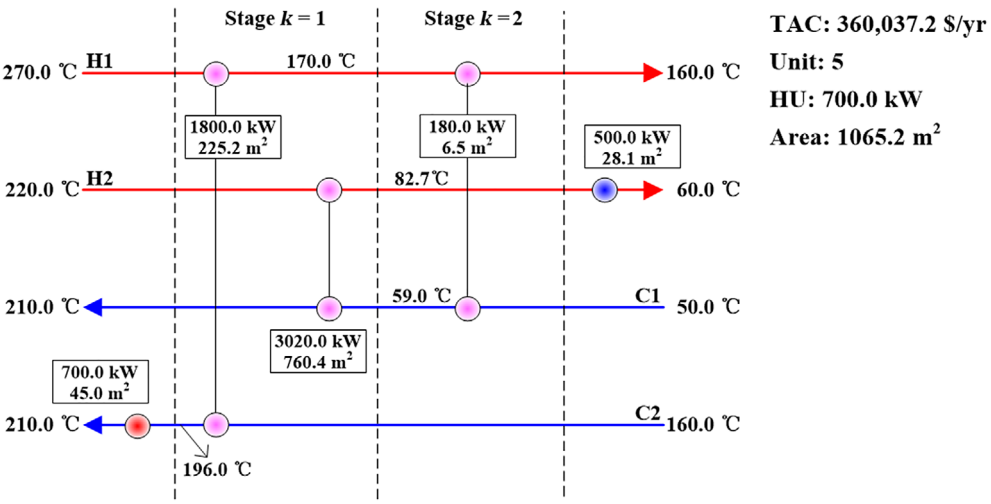

FIGURE 5 The flowsheets of optimal HEN with isothermal mixing for Example 2

effectively solve the resulting NLP (see Supporting Information-Part B) corresponding to small-size problems for each enumerated structure with fixed stream matches. In Examples 5–16, however, our Strategy 1 is slower than Strategies 2 and 3, exhibiting that the Golden Search is better than BARON in these medium- and large-scale problems. Table 2 also indicates that Strategy 3 is faster than Strategy 2, demonstrating the applicability of the proposed Lagrange Multiplier method using the KKT conditions for solving the convex NLM (*PS2*).

For illustrating purposes, we present the network designs of Example 2 in Figure 4. It includes the flowsheets of HENs with isothermal and non-isothermal mixing for the optimal structure. From Figure 4, it can be found that TAC decreases from 380,338 to 355,700 $/year (isothermal mixing vs. non-isothermal mixing). This is mainly because the hot utility demand (the energy consumption) reduces when allowing non-isothermal mixing (833.9 vs. 676.0 kW). Figure 5 shows the optimal HEN with isothermal mixing from our Part II. Comparing Figures 4(B) and 5, we find both the hot utility demand and area are decreased, resulting in 1.2% saving in TAC. In a word, it is necessary to consider non-isothermal mixing since it has certain impacts on the trade-offs between operational and capital costs for HEN synthesis. The detailed network designs of all our examples are provided in Supporting Information-Part F.

9 | CONCLUSIONS

In this work, we point out that the heat loads of heat exchangers and the stream temperatures at stages are fixed, either when fixing the energy consumption for minimal networks or when fixing the energy consumption and binding EMAT for non-minimal networks. For such two types of HENs, the NLM minimizing the area cost of heat exchangers is proved to be a convex optimization problem that we globally solve using the KKT equations. We develop new mathematical models, modified from the models proposed in Parts I and II, to include the constraints of non-isothermal mixing. Several sub-algorithms are proposed to obtain the bounds of energy consumption and the binding EMAT. Based on these, a new Global Optimum Search Algorithm is developed to obtain the globally optimal solutions for minimal and non-minimal HENs synthesis considering non-isothermal mixing.

The example tests indicate that TACs can decrease when further considering non-isothermal mixing compared to HENs synthesis with isothermal mixing. The solution comparisons verify the applicability of the proposed models and algorithms. As pointed out in the text, the proposed Strategy 3 is entirely based on mathematical programming-free procedures, except for the structure enumeration. This enumeration is done using MILMs, but can also be performed using the algorithms based on graph theory which we will study in further. New ways/methodologies will be proposed to reduce solution time and completely solve the convergence problems for large-scale examples. Another further work is to study HENs with two or more energy loops, which demand new algorithms and global search approaches.

ACKNOWLEDGMENTS

The financial supports of this research are funded by Project of National Natural Science Foundation of China (grant nos. 22008210, 21822809, and 21978256), China Postdoctoral Science Foundation (grant nos. 2020M671723 and 2019TQ0275), the Ningxia Hui Autonomous Region Key Research and Development Program (2019BFH02016). Dr. Chenglin Chang thanks the supports provided by Professor Yongrong Yang, Professor Jingdai Wang, Dr. Jingyuan Sun, and Dr. Yao Yang. André L. H. Costa thanks the National Council for Scientific and Technological Development (CNPq) for the research productivity fellowship (Process 310390/2019-2) and the financial support of the Prociência Program (UERJ). Miguel J. Bagajewicz would like to thank the Rio de Janeiro State University for its scholarship of Visiting Researcher—PAPD Program.

NOTATION

SETS

HP	set of hot process streams indexed by *i*
CP	set of cold process streams indexed by *j*
ST	set of stages indexed by *k*

PARAMETERS

$N_{\min}$	minimum number of units
NH	number of hot process streams
NC	number of cold process streams
NHU	number of hot utilities
NCU	number of cold utilities
$Y^H_{i,k}$	binary parameter representing if hot stream *i* is split or not at stage *k*
$Y^C_{j,k}$	binary parameter representing if cold stream *j* is split or not at stage *k*
$\hat{z}_{i,j,k}$	binary parameter representing if the exchanger (*i*, *j*, *k*) exists or not
$\hat{z}hu_j$	binary parameter representing if the heater of cold stream *j* exists not
$\hat{z}cu_i$	binary parameter representing if the cooler of hot stream *i* exists or not
$\hat{q}_{i,j,k}$	heat load of heat exchanger (*i*, *j*, *k*) for a MSTR or non-MSTR HENs with fixed energy consumption and the binding EMAT
$\hat{q}hu_j$	heat load of heater (*j*) for a MSTR or non-MSTR HENs with fixed energy consumption and the binding EMAT
$\hat{q}cu_i$	heat load of cooler (*i*) for a MSTR or non-MSTR HENs with fixed energy consumption and the binding EMAT
$\hat{E}$	fixed energy consumption of hot utility
$\hat{T}^H_{i,k}$	temperature of stream *i* at stage *k* upon mixing
$\hat{T}^C_{j,k}$	temperatures of stream *j* at stage *k* upon mixing
$\hat{a}$	fixed installation cost for heat exchanger
$\hat{b}$	area cost coefficient for heat exchanger
$\hat{c}$	exponent index for heat exchanger area cost
Fcp^H_i	heat capacity folwrate of hot process stream *i*
$T_{\mathrm{IN},i}$	inlet temperature of hot process stream *i*
$T_{\mathrm{OUT},i}$	outlet temperature of hot process stream *i*

Fcp_j^C heat capacity folwrate of cold process stream j
$T_{IN,j}$ inlet temperature of cold process stream j
$T_{OUT,j}$ outlet temperature of cold process stream j
$\widehat{\Omega}_i$ heat content of hot process stream i
$\widehat{\Omega}_j$ heat content of cold process stream j
$\widehat{U}_{i,j}$ overall heat transfer coefficient for exchanger between stream i and j
$\widehat{U}hu_j$ overall heat transfer coefficient for the heater of cold streams j
$\widehat{U}cu_i$ overall heat transfer coefficient for the cooler of hot streams i
$\Gamma_{i,j}$ upper bound of temperature difference for exchanger between streams i and j
Γ_j upper bound of temperature difference for the heater of stream j
Γ_i upper bound of temperature difference for the cooler of stream i
Thu^{in} inlet temperature of hot utility
Thu^{out} outlet temperature of hot utility
Tcu^{in} inlet temperature of cold utility
Tcu^{out} outlet temperature of cold utility
$\widehat{\varepsilon}$ a small number
$y_{i,j,k}^{H*}$ 1 if the binding EMAT is located at the hot end of heat exchanger (i, j, k) after running model *PLOC1S*
$y_{i,j,k}^{C*}$ 1 if the binding EMAT is located at the cold end of heat exchanger (i, j, k) after running model *PLOC1S*
yhu_j^* 1 if the binding EMAT is located at the cold end of heater (j) after running model *PLOC1S*
ycu_i^* 1 if the binding EMAT is located at the hot end of cooler (i) after running model *PLOC1S*
E^* energy consumption obtained by running model *PLOC1S*
$q_{i,j,k}^*$ heat load of heat exchanger (i, j, k) obtained by running model *PLOC1S*
qhu_j^* heat load of heater (j) obtained by running model *PLOC1S*
qcu_i^* heat load of cooler (i) obtained by running model *PLOC1S*

BINARY VARIABLES

$z_{i,j,k}$ 1 if the exchanger between streams i and j at stage k exists
zhu_j 1 if the heater of cold process stream j exists
zcu_i 1 if the cooler of hot process stream i exists
$y_{i,j,k}^H$ 1 if the temperature difference at the hot end of exchanger (i, j, k) is the smallest
$y_{i,j,k}^C$ 1 if the temperature difference at the cold end of exchanger (i, j, k) is the smallest
yhu_j 1 if the temperature difference at the cold end of heater (j) is the smallest
ycu_i 1 if the temperature difference at the hot end of cooler (i) is the smallest

CONTINUOUS VARIABLES

T temperature of hot and cold stream at stages in Synheat model
Q heat loads of heat exchangers in Synheat model
$q_{i,j,k}$ heat load of the exchanger between process streams i and j at stage k
qhu_j heat load of the heater for cold process stream j
qcu_i heat load of the cooler for hot process stream i
$T_{i,k}^H$ hot stream i temperature at stage k upon mixing
$T_{j,k}^C$ cold stream j temperature at stage k upon mixing
$f_{i,j,k}^H$ heat capacity flowrate of the split stream i exchanging heat with stream j at stage k
$f_{i,j,k}^C$ heat capacity flowrate of the split stream j exchanging heat with stream i at stage k
$t_{i,j,k}^H$ temperature of the split stream i exchanging heat with stream j at stage k
$t_{i,j,k}^C$ temperature of the split stream j exchanging heat with stream i at stage k
$\Delta t_{i,j,k}^H$ temperature difference at the hot end of heat exchanger (i, j, k)
$\Delta t_{i,j,k}^C$ temperature difference at the cold end of heat exchanger (i, j, k)
Δthu_j temperature difference at the cold end of heater j
Δtcu_i temperature difference at the hot end of cooler i
β smallest temperature difference for HEN with fixed structure
$A_{i,j,k}$ area of heat exchanger (i, j, k)
$LMTD$ logarithmic mean temperature difference
TAC_{STR} total annualized cost for a HEN with fixed structure
E_{Min}^{Iso} minimum energy for HEN structure with isothermal mixing
E_{Min}^{Niso} minimum energy for HEN structure with non-isothermal mixing
E_{Min}^{Lo} lower bound of the minimum energy for HEN with fixed structure
E_{Min}^{Up} upper bound of the minimum energy for HEN with fixed structure
E_{Max}^{Iso} maximum energy for HEN structure with isothermal mixing
E_{Max}^{Niso} maximum energy for HEN structure with non-isothermal mixing
E_{Max}^{Lo} lower bound of the maximum energy for HEN with fixed structure
E_{Max}^{Up} upper bound of the maximum energy for HEN with fixed structure
$\widehat{EMAT}_{Min}$ lower bound of the binding EMAT for HEN with fixed structure
$\widehat{EMAT}_{Max}$ upper bound of the binding EMAT for HEN with fixed structure

MODEL ACRONYM LIST

$D_{Synheat}$ Synheat model
PSTR problem rendering any viable structure of matches and candidates
PSTRR problem to enumerate different structures
PLB

	lower bound model rendering any viable structure of matches and candidates
PLBR	problem containing problem *PLB* and the exclusion constraint
PS1	non-convex model minimizing area cost for a MSTR and non-MSTR HEN with fixed energy consumption and binding EMAT
PS2	convex model minimizing area cost for a MSTR and non-MSTR HEN with fixed energy consumption and binding EMAT
PE_{Min}^{Niso}	problem targeting the minimum hot utility energy consumption
PE_{Max}^{Niso}	problem targeting the maximum hot utility energy consumption
Sy_E	system of equations for targeting energy consumption bounds
PBE_{Min}	algorithm for obtaining the lower bound of energy consumption
PBE_{Max}	algorithm for obtaining the upper bound of energy consumption
PLOC1S	problem to find the possible locations of the binding EMAT
PLOCS	problem to detect if the EMAT-binding location obtained is part of a loop
$PEMAT_{Min}^{Niso}$	problem targeting the minimum binding EMAT
$PEMAT_{Max}^{Niso}$	problem targeting the maximum binding EMAT
Sy_{EMAT}	system of equations for targeting the bounds of the binding EMAT
$PBEMAT_{Min}$	algorithm for obtaining the lower bound of the binding EMAT
$PBEMAT_{Max}$	algorithm for obtaining the upper bound of the binding EMAT

DATA AVAILABILITY STATEMENT

Data openly available in a public repository that issues datasets with DOIs

ORCID

Chenglin Chang https://orcid.org/0000-0002-1318-9530
Zuwei Liao https://orcid.org/0000-0001-9063-1049
André L. H. Costa https://orcid.org/0000-0001-9167-8754
Miguel J. Bagajewicz https://orcid.org/0000-0003-2195-0833

REFERENCES

1. Furman KC, Sahinidis NV. A critical review and annotated bibliography for heat exchanger network synthesis in the 20th century. *Ind Eng Chem Res*. 2002;41(10):2335-2370.
2. Klemeš JJ, Kravanja Z. Forty years of heat integration: pinch analysis (PA) and mathematical programming (MP). *Curr Opin Chem Eng*. 2013;2(4):461-474.
3. Nair SK, Karimi IA. Unified heat exchanger network synthesis via a Stageless superstructure. *Ind Eng Chem Res*. 2019;58(15):5984-6001.
4. Yuen A. Synthesis of performance-optimal heat exchanger networks using attainable regions. *Comput Chem Eng*. 2020;142:107043.
5. Hong X, Liao Z, Jiang B, Wang J, Yang Y. New transshipment type MINLP model for heat exchanger network synthesis. *Chem Eng Sci*. 2017;173:537-559.
6. Beck A, Hofmann R. A novel approach for linearization of a MINLP stage-wise superstructure formulation. *Comput Chem Eng*. 2018;112:17-26.
7. Nemet A, Isafiade AJ, Klemeš JJ, Kravanja Z. Two-step MILP/MINLP approach for the synthesis of large-scale HENs. *Chem Eng Sci*. 2019;197:432-448.
8. Ziyatdinov NN, Emel'yanov II, Chen Q, Grossmann IE. Optimal heat exchanger network synthesis by sequential splitting of process streams. *Comput Chem Eng*. 2020;142:107042.
9. Fieg G, Luo X, Jeżowski J. A monogenetic algorithm for optimal design of large-scale heat exchanger networks. *Chem Eng Process*. 2009;48(11):1506-1516.
10. Ravagnani MASS, Silva AP, Arroyo PA, Constantino AA. Heat exchanger network synthesis and optimisation using genetic algorithm. *Appl Therm Eng*. 2005;25(7):1003-1017.
11. Peng F, Cui G. Efficient simultaneous synthesis for heat exchanger network with simulated annealing algorithm. *Appl Therm Eng*. 2015;78:136-149.
12. Pavão LV, Costa CBB, Ravagnani MASS, Jiménez L. Large-scale heat exchanger networks synthesis using simulated annealing and the novel rocket fireworks optimization. *AIChE J*. 2017;63(5):1582-1601.
13. Silva AP, Ravagnani MASS, Biscaia EC, Caballero JA. Optimal heat exchanger network synthesis using particle swarm optimization. *Optim Eng*. 2010;11(3):459-470.
14. Huo Z, Zhao L, Yin H, Ye J. Simultaneous synthesis of structural constrained heat exchanger networks with and without stream splits. *Can J Chem Eng*. 2013;91(5):830-842.
15. Pavão LV, Costa CBB, Ravagnani MASS. Automated heat exchanger network synthesis by using hybrid natural algorithms and parallel processing. *Comput Chem Eng*. 2016;94:370-386.
16. Pavão LV, Costa CBB, Ravagnani MASS. An enhanced stage-wise superstructure for heat exchanger networks synthesis with new options for heaters and coolers placement. *Ind Eng Chem Res*. 2018;57(7):2560-2573.
17. Floudas CA, Ciric AR, Grossmann IE. Automatic synthesis of optimum heat exchanger network configurations. *AIChE J*. 1986;32(2):276-290.
18. Yee TF, Grossmann IE. Simultaneous optimization models for heat integration. II, heat exchanger network synthesis. *Comput Chem Eng*. 1990;14(10):1165-1184.
19. Zamora JM, Grossmann IE. A global MINLP optimization algorithm for the synthesis of heat exchanger networks with no stream splits. *Comput Chem Eng*. 1998;22:367-384.
20. Bergamini ML, Scenna NJ, Aguirre PA. Global optimal structures of heat exchanger networks by piecewise relaxation. *Ind Eng Chem Res*. 2007;46:1752-1763.
21. Bogataj M, Kravanja Z. An alternative strategy for global optimization of heat exchanger networks. *Appl Therm Eng*. 2012;43:75-90.
22. Faria DC, Kim SY, Bagajewicz MJ. Global optimization of the stage-wise superstructure model for heat exchanger networks. *Ind Eng Chem Res*. 2015;54(5):1595-1604.
23. Mistry M, Misener R. Optimising heat exchanger network synthesis using convexity properties of the logarithmic mean temperature difference. *Comput Chem Eng*. 2016;94:1-17.
24. Beck A, Hofmann R. How to tighten a commonly used MINLP superstructure formulation for simultaneous heat exchanger network synthesis. *Comput Chem Eng*. 2018;112:48-56.

25. Huang KF, Al-mutairi EM, Karimi IA. Heat exchanger network synthesis using a stagewise superstructure with non-isothermal mixing. *Chem Eng Sci*. 2012;73:30-43.
26. Huang KF, Karimi IA. Simultaneous synthesis approaches for cost-effective heat exchanger networks. *Chem Eng Sci*. 2013;98:231-245.
27. Huang KF, Karimi IA. Efficient algorithm for simultaneous synthesis of heat exchanger networks. *Chem Eng Sci*. 2014;105:53-68.
28. Björk KM, Westerlund T. Global optimization of heat exchanger network synthesis problems with and without the isothermal mixing assumption. *Comput Chem Eng*. 2002;26(11):1581-1593.
29. Kim SY, Bagajewicz M. Global optimization of heat exchanger networks using a new generalized superstructure. *Chem Eng Sci*. 2016;147:30-34.
30. Kim SY, Jongsuwat P, Suriyapraphadilok U, Bagajewicz M. Global optimization of heat exchanger networks. Part 1: stages/substages superstructure. *Ind Eng Chem Res*. 2017;56(20):5944-5957.
31. Chang C, Peccini A, Wang Y, Costa ALH, Bagajewicz MJ. Globally optimal synthesis of heat exchanger networks. Part I: minimal networks. *AIChE J*. 2020;66:e16267.
32. Chang C, Liao Z, Costa ALH, Bagajewicz MJ. Globally optimal synthesis of heat exchanger networks. Part II: non-minimal networks. *AIChE J*. 2020;66:e16264.
33. Paterson WR. A replacement for the logarithmic mean. *Chemical Engineering and Sciences*. 1984;39:1635.
34. Brooke A, Kendrick D, Meeraus A, Raman R. *GAMS: A Users Guide*. Washington, DC: GAMS Development; 2005.
35. Escobar M, Trierweiler JO. Optimal heat exchanger network synthesis: a case study comparison. *Appl Therm Eng*. 2013;51(1):801-826.
36. Gundersen T, Traedal P, Hashemi-Ahmady A. Improved sequential strategy for the synthesis of near-optimal heat exchanger networks. *Comput Chem Eng*. 1997;21:S59-S64.
37. Wang J, Cui G, Xiao Y, Luo X, Kabelac S. Bi-level heat exchanger network synthesis with evolution method for structure optimization and memetic particle swarm optimization for parameter optimization. *Eng Optim*. 2017;49:401-416.
38. Escobar, M, Grossmann, IE. Mixed-integer Nonlinear Programming Models for Optimal Simultaneous Synthesis of Heat Exchangers Network. Available from Cyber Infrastructure for MINLP [www.minlp.org, a collaboration of Carnegie Mellon University and IBM Research] at: www.minlp.org/library/problem/index.php?i=93. 2010.
39. Daichendt MM, Grossmann IE. Preliminary screening procedure for the MINLP synthesis of process systems-II. Heat exchanger networks. *Comput Chem Eng*. 1994;18(8):679-709.
40. Pavão LV, Costa CBB, Ravagnani MASS. A new stage-wise superstructure for heat exchanger network synthesis considering substages, sub-splits and cross flows. *Appl Therm Eng*. 2018;143:719-735.
41. Zhang H, Cui G. Optimal heat exchanger network synthesis based on improved cuckoo search via Lévy flights. *Chem Eng Res Des*. 2018;134:62-79.

SUPPORTING INFORMATION

Additional supporting information may be found in the online version of the article at the publisher's website.

How to cite this article: Chang C, Liao Z, Costa ALH, Bagajewicz MJ. Globally optimal synthesis of heat exchanger networks. Part III: Non-isothermal mixing in minimal and non-minimal networks. *AIChE J*. 2021;67(11):e17393. doi: 10.1002/aic.17393